Teleportation of position and momentum of a quantum state in terms of a correlation function of the Gaussian type: A time-dependent model

K. Saito and F.M. Toyama

Department of Information and Communication Sciences, Kyoto Sangyo University, Kyoto 603-8555, Japan

We present a time-dependent model that explicitly describes, in coordinate space, teleportation of a quantum state of position and momentum. Teleportation of an unknown quantum state is performed by means of quantum entanglement and classical communication. We assume that the quantum entanglement is expressed in terms of a correlation function of the Gaussian type that is reduced to the EPR state in the δ-function limit. We analyze an optimal situation in which a high degree of teleportation fidelity and a large teleportation probability are achieved. We also discuss a situation where the time delay due to the classical communication cannot be ignored.

1. Introduction

Bennett et al. [1] proposed a protocol of quantum teleportation of an unknown spin-1/2 state in terms of a maximally entangled spin state shared by Alice (sender) and Bob (receiver). Vaidman [2] analyzed teleportation of an unknown quantum state of continuous variables such as position and momentum in terms of the EPR (Einstein, Podlsky and Rosen) state [3] that represents perfect correlations in both variables. Braunstein and Kimble [4] extended Vaidman's analysis to incorporate incomplete correlations in both variables and inefficiencies in the measurement process. They also provided a scheme for realistic implementation of teleportation of continuous variables, using quadrature amplitudes of the electromagnetic field. Furusawa et al. [5] examined experimentally such a scheme.

The protocol of quantum teleportation consists of three ingredients, i.e., a quantum entangled state that is shared by Alice and Bob, an entangle-measurement by Alice and a unitary transformation of a state generated at Bob's site. In order to perform the unitary transformation Bob has to know the results of the measurement done by Alice. Therefore, Alice informs Bob of the results of her measurement by classical communication. The classical communication is an indispensable part of the protocol. However, Bob cannot always restore the same state as the input state by the unitary transformation. This inefficiency of the teleportation is mainly due to the incompleteness of the entanglement and the measurement process. Here, we point out that there exists another factor that causes inefficiency in the teleportation. A time delay due to classical communication allows the post-measurement state generated at Bob's site to develop over time. In a situation where the time-evolution of the post-measurement state before the unitary transformation is not negligible, we have to take account of such time-evolution of the post-measurement state.

The purpose of the present work is to investigate such inefficiencies in quantum teleportation of continuous variables. For this purpose we present a time-dependent model that explicitly describes, in coordinate space, the process of the teleportation of momentum and position.

2. A time-dependent model

We consider three particles that we designate as 1, 2 and 3, respectively. Alice and Bob share an entangled state $|\psi_{23}(t)\rangle$ of particles 2 and 3. To teleport an input state $|\psi_1(t)\rangle$ of particle 1 to Bob, Alice does the measurements of two commutative observables $\hat{X}_{12} = \hat{x}_1 + \hat{x}_2$ and $\hat{P}_{12} = \hat{p}_1 - \hat{p}_2$ of particles 1 and 2, where $\hat{x}_i$ and $\hat{p}_i$ $(i = 1,2)$ are respectively the position and momentum operators of each particle. When Alice does the measurements of $\hat{X}_{12}$ and $\hat{P}_{12}$, a state $|\psi_3(t)\rangle$ of particle 3 is generated at Bob's site. Except for a special case, the generated state $|\psi_3(t)\rangle$ is different from the input state $|\psi_1(t)\rangle$. In order to complete the teleportation, Bob has to transform $|\psi_3(t)\rangle$ to $|\psi_1(t)\rangle$. The transformation is realized by a unitary operator that is determined with the results of the measurements of $\hat{X}_{12}$ and $\hat{P}_{12}$. Alice informs Bob of the results of her measurement by classical communication so that Bob can perform the unitary transformation.

For the unknown input state $|\psi_1(t)\rangle$, which Alice wants to teleport to Bob, we take it as

$$|\psi_1(t)\rangle = N_{1m}\left[\,\left|\phi_1^+(t)\right\rangle + \left|\phi_1^-(t)\right\rangle\,\right], \tag{2.1}$$

where $|\phi_1^\pm(t)\rangle$ are normalized to unity and N_{1m} is the renormalization factor. For $|\phi_1^\pm(t)\rangle$ we take them in coordinate representation as

$$\phi_1^\pm(x_1,t) = \langle x_1|\phi_1^\pm(t)\rangle = \frac{N_1}{\sqrt{1+\dfrac{i\hbar t}{m\sigma_1^2}}}\exp\left\{-\frac{\left(x_1 - x_0^\pm - \dfrac{\hbar K^\pm}{m}t\right)^2}{2\sigma_1^2\left(1+\dfrac{i\hbar t}{m\sigma_1^2}\right)} + i\left[K^\pm\left(x_1 - x_0^\pm\right) - \frac{\hbar K^{\pm 2}}{2m}t\right]\right\}, \tag{2.2}$$

where $N_1 = (\pi\sigma_1^2)^{-1/4}$ is the normalization factor, m is the mass of particle 1, σ_1 and $K^\pm$ are respectively the width and wave numbers of the wave packets $\phi_1^\pm(x_1,t)$. The wave packets $\phi_1^\pm(x_1,t)$ are solutions of the free Schrödinger equation. In numerical illustrations we will take $K^\pm$ as $K^+ = -K^-$. For such a choice of $K^\pm$, the input state $|\psi_1(t)\rangle$ is a two-mode state. For Eq. (2.2) the renormalization factor N_{1m} is given as

$$N_{1m} = \left\{2\left[1+\exp\left(-\frac{\left(x_0^+ - x_0^-\right)^2}{4\sigma_1^2} - \frac{\sigma_1^2\left(K^+ - K^-\right)^2}{4}\right)\cos\left(\frac{\left(K^+ - K^-\right)\left(x_0^- - x_0^+\right)}{2}\right)\right]\right\}^{-\frac{1}{2}}. \tag{2.3}$$

The Wigner distribution [6] of the input state is expressed as

$$W_{in}(x_1,p_1,t) = \frac{1}{2\pi\hbar}\int_{-\infty}^{\infty} dy\,\exp\left(i\frac{p_1 y}{\hbar}\right)\left\langle x_1 + \frac{y}{2}\left|\hat{\rho}_1(t)\right|x_1 - \frac{y}{2}\right\rangle, \tag{2.4}$$

where $\hat{\rho}_1(t)$ is the density matrix of the input state, i.e., $\hat{\rho}_1(t) = |\psi_1(t)\rangle\langle\psi_1(t)|$. The Wigner distribution (2.4) is useful in seeing the quantum coherence in $|\psi_1(t)\rangle$.

Next, we consider the measurement sate for Alice. We suppose that Alice does her measurements of two commutative observables $\hat{X}_{12} = \hat{x}_1 + \hat{x}_2$ and $\hat{P}_{12} = \hat{p}_1 - \hat{p}_2 =$

$-i\hbar\left(\partial/\partial x_1 - \partial/\partial x_2\right)$ at $t = 0$. In our model we represent the measurement state at $t = 0$ as

$$\chi_{a,b}(x_1,x_2) = \left\langle x_1 x_2 \big| \chi_{a,b} \right\rangle$$

$$= N_{12} \exp\left[-\frac{1}{2\sigma_{12}^2}(x_1 + x_2 - a)^2 - \frac{1}{2\sigma_{12r}^2}(x_1 - x_2)^2 + i(k_1 x_1 + k_2 x_2) \right], \quad (2.5)$$

where σ_{12} and σ_{12r} are respectively the distribution parameters of the center-of-mass and relative motions, k_1 and k_2 are the averaged wave numbers of particles 1 and 2, $b = k_1 - k_2$ and $N_{12} = \left(2/\pi\sigma_{12}\sigma_{12r}\right)^{1/2}$ is the normalization factor. In terms of Eq. (2.5) the expectation values of $\hat{X}_{12}$ and $\hat{P}_{12}$ are given as

$$\left\langle \chi_{a,b} \big| \hat{X}_{12} \big| \chi_{a,b} \right\rangle = a \quad \text{and} \quad \left\langle \chi_{a,b} \big| \hat{P}_{12} \big| \chi_{a,b} \right\rangle = \hbar(k_1 - k_2) = \hbar b. \quad (2.6)$$

For $\{\sigma_{12} \to$ very small, $\sigma_{12r} \to$ very large$\}$, two equations of Eq. (2.6) approach the following approximate eigenvalue equations, i.e., $\hat{X}_{12} \big| \chi_{a,b} \rangle = a \big| \chi_{a,b} \rangle$ and $\hat{P}_{12} \big| \chi_{a,b} \rangle = \hbar b \big| \chi_{a,b} \rangle$. Here, the perfect limit of $\{\sigma_{12} \to 0, \sigma_{12r} \to \infty\}$ is not physical in the sense that Eq. (2.5) approaches a measurement state of the δ-function type with an infinitely small normalization factor $2(\sigma_{12}/\sigma_{12r})^{1/2}$ in the limit.

Here let us consider the correlation state $\big| \psi_{23}(t) \rangle$ between particles 2 and 3, which is shared by Alice and Bob. We assumed that Alice does her measurements at $t = 0$. Therefore, in fact we need $\big| \psi_{23}(t = 0) \rangle$. For the correlation at $t = 0$ we assume the Gaussian type,

$$\psi_{23}(x_2,x_3,t=0) = \left\langle x_2 x_3 \big| \psi_{23}(t=0) \right\rangle$$

$$= N_{23} \exp\left[-\frac{(x_2 + x_3)^2}{2\sigma_{23}^2} - \frac{(x_2 - x_3)^2}{2\sigma_{23r}^2} + ik_{23}(x_2 + x_3) + ik_{23r}(x_2 - x_3) \right], \quad (2.7)$$

where σ_{23} and σ_{23r} are the distribution parameters of the center-of-mass and relative motions of the two particles, k_{23} and k_{23r} are the wave numbers for the center-of-mass and relative motions and $N_{23} = \left(2/\pi\sigma_{23}\sigma_{23r}\right)^{1/2}$ is the normalization factor. If $\sigma_{23} = \sigma_{23r}$, Eq. (2.7) has no correlation between x_2 and x_3. In fact, we examine cases where σ_{23} is very small and σ_{23r} is very large. Further, Eq. (2.7) has no correlation for the center-of-mass and relative coordinates $(x_2 + x_3)/2$ and $x_2 - x_3$. When $k_{23r} \neq 0$, Eq. (2.7) is neither symmetric nor anti-symmetric for the exchange of particles 2 and 3. Therefore, in numerical illustrations we will take k_{23r} to be 0. The expectation values of two commutative observables $\hat{X}_{23} = \hat{x}_2 + \hat{x}_3$ and $\hat{P}_{23} = \hat{p}_2 - \hat{p}_3$ in terms of Eq. (2.7) are

$$\left\langle \psi_{23}(t=0) \big| \hat{X}_{23} \big| \psi_{23}(t=0) \right\rangle = 0 \quad \text{and} \quad \left\langle \psi_{23}(t=0) \big| \hat{P}_{23} \big| \psi_{23}(t=0) \right\rangle = 2\hbar k_{23r}. \quad (2.8)$$

In the limit of $\{\sigma_{23} \to$ very small, $\sigma_{23r} \to$ very large$\}$, Eq. (2.8) can be regarded as approximate eigenvalue equations $\hat{X}_{23} \big| \psi_{23} \rangle = 0 \big| \psi_{23} \rangle$ and $\hat{P}_{23} \big| \psi_{23} \rangle = 2\hbar k_{23r} \big| \psi_{23} \rangle$. Here, the perfect limit of $\{\sigma_{23} \to 0, \sigma_{23r} \to \infty\}$ is not physical because Eq. (2.8) approaches a correlation function of the δ-function type with the infinitely small normalization factor $2(\sigma_{23}/\sigma_{23r})^{1/2}$ in the limit.

When Alice does the measurements of $\hat{X}_{12}$ and $\hat{P}_{12}$ at $t = 0$, a state $\big| \psi_3(t=0) \rangle$ of particle 3 is instantaneously generated at Bob's site. Here, note that our model is a non-relativistic model.

We call the generated state the post-measurement state hereafter. We describe the measurement process as

$$\left\langle \chi_{a,b} \left| \psi_1(t=0) \otimes \psi_{23}(t=0) \right\rangle \right|_{12} = \varsigma \left| \psi_3(t=0) \right\rangle, \tag{2.9}$$

where ς is the probability amplitude for generating $\left| \psi_3(t=0) \right\rangle$. The post-measurement state $\left| \psi_3(t=0) \right\rangle$ consists of two components, i.e.,

$$\left| \psi_3(t=0) \right\rangle = N_{3m} \left[\left| \phi_3^+(t=0) \right\rangle + \left| \phi_3^-(t=0) \right\rangle \right], \tag{2.10}$$

where N_{3m} is the normalization factor. By using Eqs. (2.1), (2.5) and (2.7) the component states $\left| \phi_3^\pm(t=0) \right\rangle$ in Eq. (2.10) can explicitly be given in coordinate space as

$$\phi_3^\pm(x_3, t=0) = \left\langle x_3 \left| \phi_3^\pm(t=0) \right\rangle \right.$$

$$= \exp\left[L_0^\pm + \frac{L_1^{\pm 2}}{L_2} + i\left(\frac{M_1^\pm L_1^\pm}{L_2} + M_0^\pm \right) \right] \exp\left[-L_2\left(x_3 - \frac{L_1^\pm}{L_2} \right)^2 + iM_1^\pm\left(x_3 - \frac{L_1^\pm}{L_2} \right) \right], \tag{2.11}$$

where $L_0^\pm = I^{\pm 2}/H + (Aa + Cx_0^\pm)^2/F - k_a^{\pm 2}/F - (k_b - k_a^\pm G/F)^2/4H - Aa^2 - Cx_0^{\pm 2}$, $L_1^\pm = 2I^\pm J/H$, $L_2 = D + E - J^2/H$, $M_0^\pm = -K^\pm x_0^\pm + k_a^\pm (Aa - Cx_0^\pm)/F - I^\pm (k_b - k_a^\pm G/F)/H$ and $M_1^\pm = J(k_c - k_b + k_a^\pm G/F)/H$ with $A = 1/2\sigma_{12}^2$, $B = 1/2\sigma_{12r}^2$, $C = 1/2\sigma_1^2$, $D = 1/2\sigma_{23}^2$, $E = 1/2\sigma_{23r}^2$, $F = A + B + C$, $G = A - B$, $H = A + B + D + E - G^2/F$, $I^\pm = G\left(Aa + C x_0^\pm \right)/F - Aa$, $J = D - E$, $k_a^\pm = K^\pm - k_1$, $k_b = k_{23}$ $+ k_{23r} - k_2$ and $k_c = k_{23} - k_{23r}$. For $\phi_3^\pm$ of Eq. (2.11) N_{3m} is given as

$$N_{3m} = \left\{ \sqrt{\frac{\pi}{2L_2}} \left[\exp\left(2\left(L_0^+ + \frac{L_1^{+2}}{L_2} \right) \right) + \exp\left(2\left(L_0^- + \frac{L_1^{-2}}{L_2} \right) \right) \right. \right.$$

$$\left. \left. + 2\exp\left(L_0^+ + L_0^- + \frac{1}{2L_2}(L_1^+ + L_1^-)^2 - \frac{1}{8L_2}(M_1^+ - M_1^-)^2 \right) \cos\left(\frac{(M_1^+ - M_1^-)(L_1^+ + L_1^-)}{2L_2} + M_0^+ - M_0^- \right) \right] \right\}^{-\frac{1}{2}}. \tag{2.12}$$

By using Eqs. (2.1), (2.5) and (2.7), from Eqs. (2.9) and (2.10) the generation probability can be obtained as

$$\left| \varsigma \right|^2 = \left(\frac{\pi N_1 N_{12} N_{23} N_{1m}}{\sqrt{FH} N_{3m}} \right)^2. \tag{2.13}$$

The $\left| \varsigma \right|^2$ is a function of parameters σ_1, σ_{12}, σ_{12r}, σ_{23}, σ_{23r}, $K^\pm$, $x_0^\pm$, a, k_1, k_2, k_{23} and k_{23r}. The post-measurement state $\left| \psi_3(t=0) \right\rangle$ of Eq. (2.10) is different from the input state $\left| \psi_1(t=0) \right\rangle$, except for a special case where the correlation between particles 2 and 3 is the δ-function type and the results of the measurement of $\hat{X}_{12}$ and $\hat{P}_{12}$ are both 0. In order to complete the teleportation Bob has to transform $\left| \psi_3(t=0) \right\rangle$ into $\left| \psi_3^{tel}(t) \right\rangle$ by a unitary transformation $\hat{U}(a,b)$ that is constructed with the results of the measurement a and $\hbar b$. Alice informs the results of

her measurements a and $\hbar b$ to Bob using classical communication. This classical communication causes a time delay. In a situation where we cannot ignore such a time delay we have to take into account the time-evolution of the post-measurement state. If we suppose that the post-measurement state evolves in free space, we can write down the time-evolution of the post-measurement state of Eq. (2.10) analytically as

$$\left| \psi_3(t) \right\rangle = N_{3rn} \left[\left| \phi_3^+(t) \right\rangle + \left| \phi_3^-(t) \right\rangle \right] ,$$ (2.14)

where

$$\phi_3^{\pm}(x_3,t) = \left\langle x_3 \left| \phi_3^{\pm}(t) \right\rangle \right. = \frac{1}{\sqrt{1 + i\frac{2L_2\hbar t}{m}}} \exp\left[L_0^{\pm} + \frac{L_1^{\pm 2}}{L_2} + i\left(\frac{M_1^{\pm}L_1^{\pm}}{L_2} + M_0^{\pm} \right) \right]$$

$$\times \exp\left\{ -\frac{L_2\left(x_3 - \frac{L_1^{\pm}}{L_2} - v_0^{\pm}t \right)^2}{1 + i\frac{2L_2\hbar t}{m}} + i\left[M_1^{\pm}\left(x_3 - \frac{L_1^{\pm}}{L_2} \right) - \omega_0^{\pm}t \right] \right\}.$$ (2.15)

In Eq. (2.15), $v_0^{\pm} = \hbar M_1^{\pm}/m$ and $\omega_0^{\pm} = \hbar M_1^{\pm 2}/2m$. The wave functions (2.15) are solutions of the free Schrödinger equation.

The unitary transformation $\hat{U}(a,b)$ is expressed in coordinate space as

$$\hat{U}_x(a,b,x_3) = \left\langle x_3 \left| \hat{U}(a,b) \right| x_3 \right\rangle = \exp\left\{ i\left[(b + 2k_{23r})\hat{x}_3 - \frac{a\hat{p}_3}{\hbar} \right] \right\} \exp\left(iak_1 \right),$$ (2.16)

where $\hat{p}_3 = -i\hbar \, \partial/\partial x_3$. The constant phase factor $\exp(iak_1)$ in Eq. (2.16) arises in the δ-function limit of $\left| \psi_{23}(t) \right\rangle$ and $\left| \chi_{a,b} \right\rangle$ [2].

The Wigner distribution of the post-measurement state $\left| \psi_3(t) \right\rangle$ is expressed as

$$W_{out}(x_3,p_3,t) = \frac{1}{2\pi\hbar} \int_{-\infty}^{\infty} dy \, \exp\left(i\frac{p_3 y}{\hbar} \right) \left\langle x_3 + \frac{y}{2} \left| \hat{\rho}_3(t) \right| x_3 - \frac{y}{2} \right\rangle,$$ (2.17)

where $\hat{\rho}_3(t) = \left| \psi_3(t) \right\rangle\left\langle \psi_3(t) \right|$. For the Wigner distribution $W_{out}(x_3,p_3, t)$ of Eq. (2.17), the unitary transformation $\hat{U}(a,b)$ of Eq. (2.16) is just the shift operation $\{ x_3 \rightarrow x_3 - a$, $p_3 \rightarrow p_3 - \hbar(b + 2k_{23r}) \}$, namely $W_{out}^{tel}(x_3,p_3,t) = W_{out}(x_3 - a, p_3 - \hbar(b + 2k_{23r}), t)$. The fidelity $F(t)$ of the teleportation is defined as

$$F(t) = \left\langle \psi_1(t = 0) \left| \hat{\rho}_{out}^{tel}(t) \right| \psi_1(t = 0) \right\rangle,$$ (2.18)

where $\hat{\rho}_{out}^{tel}(t) = \left| \psi_3^{tel}(t) \right\rangle\left\langle \psi_3^{tel}(t) \right|$.

3. Numerical illustrations

In numerical illustrations we assume that m is the electron mass and use atomic units. Then $m = 1$, $\hbar = 1$ and $c = 137$. The unit length is the Bohr radius. Figure 1 shows the Wigner distribution $W_{in}(x_1, p_1, t = 0)$ of the input state $|\psi_1(t = 0)\rangle$ of Eq. (2.1). For the parameters of the input state we took them to be $\sigma_1 = 5$, $x_0^+ = -5$, $x_0^- = -7$ and $K^\pm = \pm 0.5$. The distribution $W_{in}(x_1, p_1, t = 0)$ has an oscillation with negative distribution between the two positive distributions around $p_1 = \pm 5$. This represents quantum coherence due to the terms $|\phi_1^+(t = 0)\rangle\langle\phi_1^-(t = 0)|$ and $|\phi_1^-(t = 0)\rangle\langle\phi_1^+(t = 0)|$ in $\hat{\rho}_1(t = 0)$.
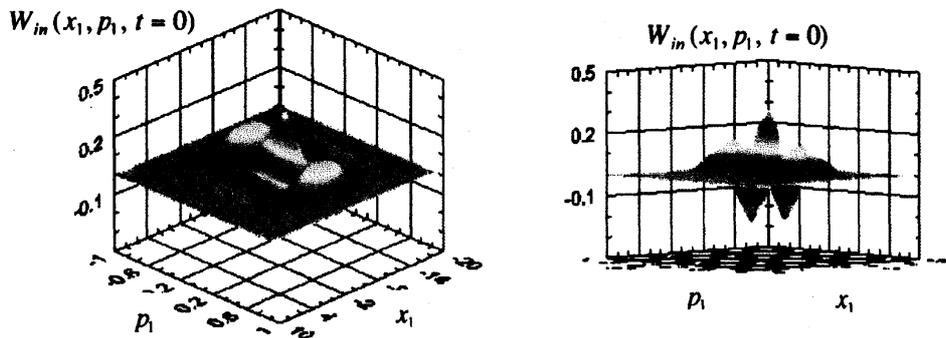
Fig.1 The Wigner distribution $W_{in}(x_1, p_1, t = 0)$ of the input state $|\psi_1(t = 0)\rangle$ of Eq. (2.1). The parameters of the input state are taken as $\sigma_1 = 5$, $K^\pm = \pm 0.5$, $x_0^+ = -5$, $x_0^- = -7$ and $m = 1$. The units are atomic units.
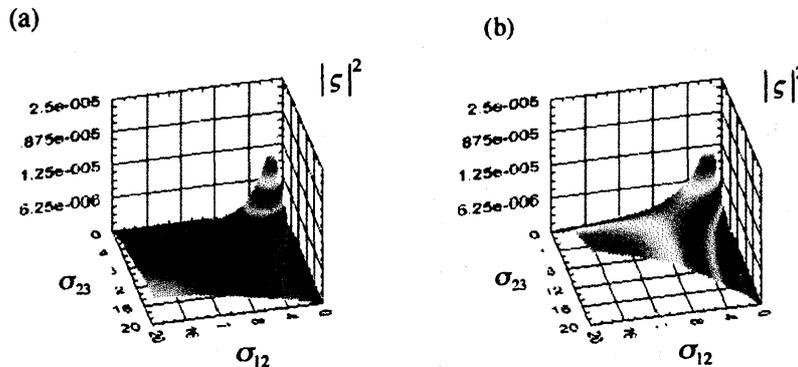
Fig. 2 The behavior of the generating probability $|\varsigma|^2$ for the parameters σ_{12} and σ_{23}. (a) shows the case of $b = 0$ ($k_1 = k_2 = 0$). The position of the maximum is $\sigma_{12} = \sigma_{23} = 1.65$. (b) shows the case of $b = 0.1$ ($k_1 = 0.1$, $k_2 = 0$). The position of the maximum is $\sigma_{12} = \sigma_{23} = 1.87$. The other parameters are taken as $\sigma_{12r} = \sigma_{23r} = 10^3$, $K^\pm = \pm 0.5$, $x_0^+ = -5$, $x_0^- = -7$, $k_{12} = k_{23} = 0$ and $a = 2$. The units are atomic units.

First, we examine the generation probability $|\varsigma|^2$ of the state $|\psi_3(t = 0)\rangle$. Figure 2 exhibits the behavior of $|\varsigma|^2$ for the parameters σ_{12} and σ_{23} that represent distributions of the center-of-mass motions in the measurement and the correlation state. Figure 2a is the case where the results of measurement by Alice are assumed to be $a = \hbar b = 0$. The generation probability $|\varsigma|^2$ is very small as a whole. For smaller σ_{12r} and σ_{23r}, $|\varsigma|^2$ becomes larger. However, the smaller σ_{12r} and σ_{23r} are, the smaller the fidelity becomes. Therefore, in Fig. 2 we fixed the parameters σ_{12r} and σ_{23r} to be 10^3 to get a high fidelity. An interesting feature of $|\varsigma|^2$ is that it has a local

maximum in a small $(\sigma_{12},\sigma_{23})$ region. The position of the local maximum is around $(\sigma_{12},\sigma_{23}) \approx (1.65, 1.65)$ for the case of $a = \hbar b = 0$. Figure 2b illustrates the shift of the position of the maximum for b. As the shift of the local maximum is not sensitive to a, we fixed it to be 2 in the illustration. The local maximum shifts to a larger region of σ_{12} and σ_{23} for larger b. For $b \geq 0.2$ the maximum in the small $(\sigma_{12},\sigma_{23})$ region disappears and around $b \approx 0.8$ it reappears. Actually there exists a big bump in a very large $(\sigma_{12},\sigma_{23})$ region. For $0.2 \leq b \leq 0.8$, the bump in such a large $(\sigma_{12},\sigma_{23})$ region masks the local maximum in the small $(\sigma_{12},\sigma_{23})$ region.

(a) $W_{out}^{tel}(x_3,p_3,t=0)$

$W_{out}^{tel}(x_3,p_3,t=0)$

(b) $W_{out}^{tel}(x_3,p_3,t=4)$
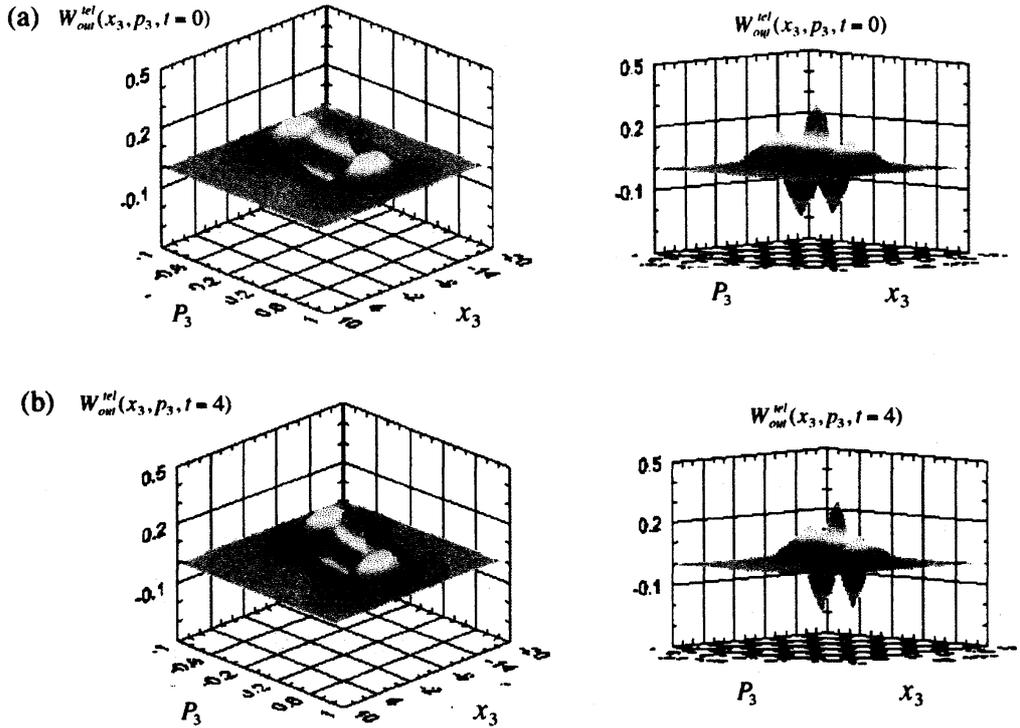
$W_{out}^{tel}(x_3,p_3,t=4)$

Fig. 3 (a) The Wigner distribution $W_{out}^{tel}(x_3,p_3,t=0)$ of the output state $|\psi_3^{tel}(t=0)\rangle = \hat{U}(a=2,b=0.1)|\psi_3(t=0)\rangle$. The fidelity is $F(t=0)=0.999$. (b) The Wigner distribution $W_{out}^{tel}(x_3,p_3,t=4)$ of the output state $|\psi_3^{tel}(t=4)\rangle = \hat{U}(a=2,b=0.1)|\psi_3(t=4)\rangle$. The Fidelity is $F(t=4)=0.885$. The results of the measurement by Alice are assumed to be $a=2$, $b=0.1$ ($k_1=0.1$, $k_2=0$). The parameters of $|\chi_{a,b}\rangle$ and $|\psi_{23}\rangle$ are $k_{23}=k_{23r}=0$, $\sigma_{12r}=\sigma_{23r}=10^3$ and $\sigma_{12}=\sigma_{23}=10^{-3}$. The units are atomic units.

Figure 3a shows the Wigner distribution $W_{out}^{tel}(x_3,p_3,t=0)$ of the output state $|\psi_3^{tel}(t=0)\rangle$, where $a=2$ and $b=0.1$ ($k_1=0.1$, $k_2=0$); $b=0.1$ corresponds to $1/1370$ of c. Other parameters of $|\psi_{23}\rangle$ and $|\chi_{a,b}\rangle$ are taken to be $k_{23}=k_{23r}=0$, $\sigma_{12r}=\sigma_{23r}=10^3$ and $\sigma_{12}=\sigma_{23}=10^{-3}$. Note that σ_{12r} and σ_{23r} are very large and σ_{12} and σ_{23} are very small. This choice of the parameters σ_{12r}, σ_{23r}, σ_{12} and σ_{23} gives a situation close to the δ-function limit of the measurement and correlation states. As seen in the figure $W_{out}^{tel}(x_3,p_3,t=0)$ is almost the same as $W_{in}(x_1,p_1,t=0)$ of the input state. The fidelity is very high in this case, i.e., $F(t=0)=0.999$, as expected. The teleportation in this situation seems quite successful. However, as seen in Fig. 2b the generation probability $|\varsigma|^2$ is very small in this case. Thus, although we can achieve teleportation with high fidelity by supposing a situation close to the δ-function limit of the measurement and correlation states, we have to give up obtaining a high teleportation probability.

Figure 3b exhibits $W_{out}^{tel}(x_3, p_3, t=4)$, which illustrates the time-evolution of the post-measurement state $|\psi_3^{tel}(t=4)\rangle$. As a typical case we have shown the case of $t=4$ ($\approx 9.676 \times 10^{-17}$ s). The difference between $W_{out}^{tel}(x_3, p_3, t=4)$ and $W_{out}^{tel}(x_3, p_3, t=0)$ is appreciable. The fidelity at $t=4$ is $F(t=4)=0.885$, which is much reduced from $F(t=0)=0.999$. Thus, in the present analysis, the effect of the time-evolution of the post-measurement state before the unitary transformation becomes appreciable around $t=4$.
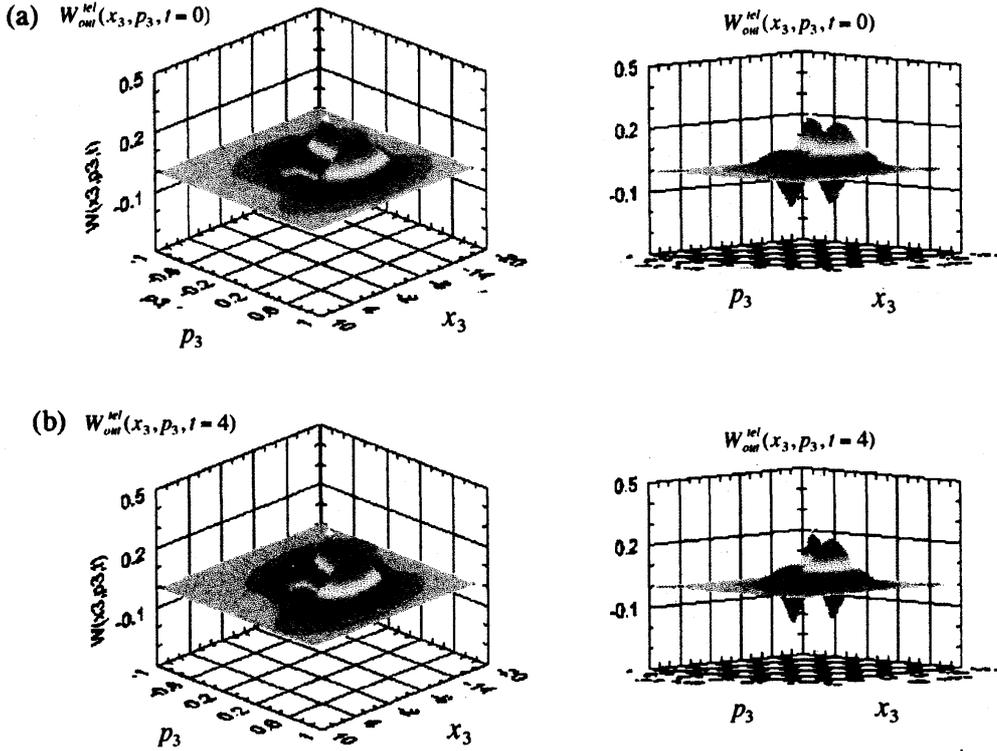
Fig. 4 (a) The Wigner distribution $W_{out}^{tel}(x_3, p_3, t=0)$ of the output state $|\psi_3^{tel}(t=0)\rangle = \hat{U}(a=2, b=0.1)|\psi_3(t=0)\rangle$ for $\sigma_{12}=\sigma_{23}=1.87$. The fidelity is $F(t=0)=0.793$. (b) The Wigner distribution $W_{out}^{tel}(x_3, p_3, t=4)$ of the output state $|\psi_3^{tel}(t=4)\rangle = \hat{U}(a=2, b=0.1)|\psi_3(t=4)\rangle$ for $\sigma_{12}=\sigma_{23}=1.87$. The fidelity is $F(t=4)=0.737$. Other parameters are the same as those of Fig. 3. The units are atomic units.

Next, we consider a situation that corresponds to the local maximum of $|\varsigma|^2$ in the small $(\sigma_{12}, \sigma_{23})$ region. The $|\varsigma|^2$ has the local maximum around $(\sigma_{12}, \sigma_{23}) \approx (1.87, 1.87)$ for $a=2$ and $b=0.1$ ($k_1=0.1$, $k_2=0$) (see Fig. 2b). Figures 4a and 4b show the outputs $W_{out}^{tel}(x_3, p_3, t=0)$ and $W_{out}^{tel}(x_3, p_3, t=4)$ for $\sigma_{12}=\sigma_{23}=1.87$, respectively. The other parameters are the same as those of Fig. 3. The $W_{out}^{tel}(x_3, p_3, t=0)$ and $W_{out}^{tel}(x_3, p_3, t=4)$ are both considerably different from $W_{in}(x_1, p_1, t=0)$ of the input state (see Fig. 1). The fidelity is $F(t=0)=0.793$ and $F(t=4)=0.737$. In this case the generation probability is orders-of-magnitude larger than that of Fig. 3. However, the fidelity is much reduced. This is because σ_{12} and σ_{23} are very large compared with those of Fig. 3. Thus, in order to obtain a high generation probability we have to compromise on the reduction of the fidelity.

So far we have kept σ_{12}, and σ_{23}, very large, i.e., $\sigma_{12}=\sigma_{23}=10^3$. For very small σ_{12} and σ_{23}, this gives a situation close to the δ-function limit of the measurement and correlation states. Here we examine a case where σ_{12}, and σ_{23}, are both considerably small. As an example, in Fig.

5 we show $|\varsigma|^2$ for $\sigma_{12r} = \sigma_{23r} = 20$, where other parameters of the measurement and correlation states are the same as those of Fig. 3. The $|\varsigma|^2$ is very large as a whole compared with that of Fig. 2b in which $\sigma_{12r} = \sigma_{23r} = 10^3$. The position of the local maximum of $|\varsigma|^2$ is around $(\sigma_{12}, \sigma_{23}) = (2.01, 2.03)$. Figures 6a and 6b show the outputs $W_{out}^{tel}(x_3, p_3, t = 0)$ and $W_{out}^{tel}(x_3, p_3, t = 4)$ for $(\sigma_{12}, \sigma_{23}) = (2.01, 2.03)$, respectively. In this case, the outputs $W_{out}^{tel}(x_3, p_3, t = 0)$ and $W_{out}^{tel}(x_3, p_3, t = 4)$ are both quite different from the input $W_{in}(x_1, p_1, t = 0)$. The fidelity is small, i.e., $F(t = 0) = 0.621$ and $F(t = 4) = 0.567$. Although we can obtain a large generation probability by taking σ_{12r} and σ_{23r} to be small, we have to give up obtaining a high degree of fidelity.
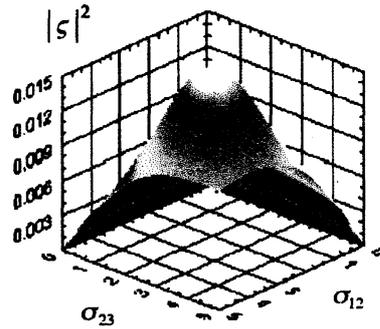
Fig. 5 The generation probability $|\zeta|^2$ of the state $|\psi_3(t = 0)\rangle$. The parameters are taken as $\sigma_{12r} = \sigma_{23r} = 20$, $a = 2$, $b = 0.1$ ($k_1 = 0.1$, $k_2 = 0$). The other parameters are the same as those of Fig. 3. The position of the maximum is around $(\sigma_{12}, \sigma_{23}) = (2.01, 2.03)$. The units are atomic units.

(a) $W_{out}^{tel}(x_3, p_3, t = 0)$

$W_{out}^{tel}(x_3, p_3, t = 0)$
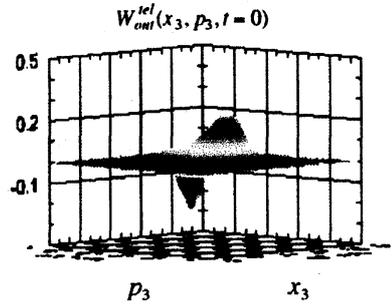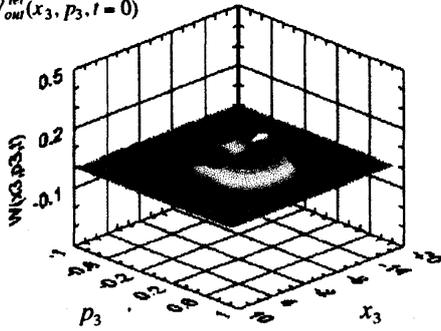
(b) $W_{out}^{tel}(x_3, p_3, t = 4)$
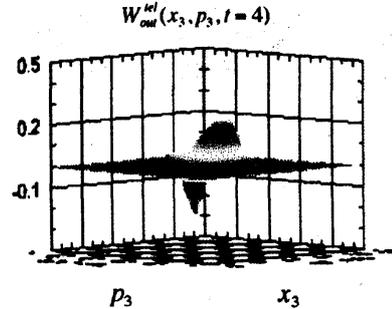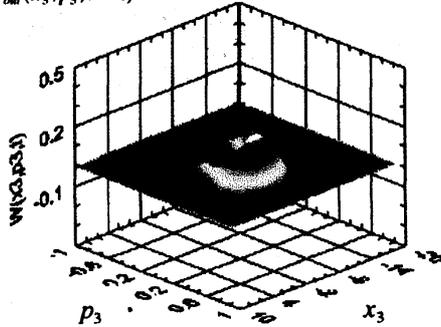
$W_{out}^{tel}(x_3, p_3, t = 4)$

Fig. 6 (a) The Wigner distribution $W_{out}^{tel}(x_3, p_3, t = 0)$ of the output state $|\psi_3^{tel}(t = 0)\rangle = U(a = 2, b = 0.1)|\psi_3(t = 0)\rangle$ for $(\sigma_{12}, \sigma_{23}) = (2.01, 2.03)$. The fidelity is $F(t = 0) = 0.621$. (b) The Wigner distribution $W_{out}^{tel}(x_3, p_3, t = 4)$ of $|\psi_3^{tel}(t = 4)\rangle = U(a = 2, b = 0.1)|\psi_3(t = 4)\rangle$ for $(\sigma_{12}, \sigma_{23}) = (2.01, 2.03)$. The fidelity is $F(t = 4) = 0.567$. The parameters σ_{12r} and σ_{23r} are taken as $\sigma_{12r} = \sigma_{23r} = 20$. Other parameters are the same as those of Fig. 3. The units are atomic units.

Finally, we consider a special case that illustrates the classical limit of the quantum teleportation. Figure 7 shows the output $W_{out}^{tel}(x_3,p_3,t=0)$ for the parameters $\sigma_{12}=\sigma_{23}=1.365$, $\sigma_{12r}=\sigma_{23r}=10^3$, $a=2$ and $b=1$ ($k_1=1,k_2=0$). Note that b is taken to be very large. The input state is the same as that of Fig. 1, namely the two-mode state of Eq. (2.1). As seen in Fig.7, the quantum coherence has almost disappeared in the output $W_{out}^{tel}(x_3,p_3,t=0)$. Moreover, one of the two modes of the input state has been almost transferred to another mode. This situation can be clarified by comparing the $W_{out}^{tel}(x_3,p_3,t=0)$ with the Wigner distribution of the output state for the one-mode input state $|\psi_1(t)\rangle=|\phi_1^+(t)\rangle$. Figure 8a shows the Wigner distribution $W_{in}(x_1,p_1,t=0)$ of the one-mode input state $|\psi_1(t)\rangle=|\phi_1^+(t)\rangle$. Figure 8b is the output $W_{out}^{tel}(x_3,p_3,t=0)$ for this input state. The output $W_{out}^{tel}(x_3,p_3,t=0)$ of Fig. 7 is very similar to the output $W_{out}^{tel}(x_3,p_3,t=0)$ of Fig. 8b. The fidelity in this case is $F(t=0)=0.5005$, which is very close to $F=0.5$ for the classical limit of quantum teleportation. This implies that the result shown in Fig. 7 represents a situation close to the classical limit of the quantum teleportation.
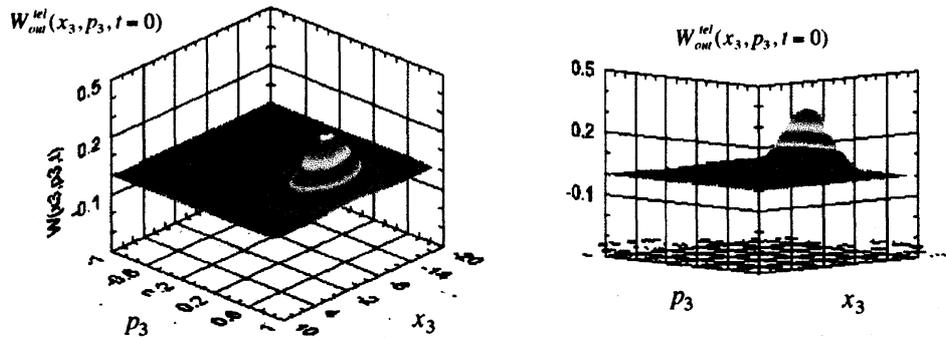
Fig. 7 The Wigner distribution $W_{out}^{tel}(x_3,p_3,t=0)$ of the output state $|\psi_3^{tel}(t=0)\rangle=\hat{U}(a=2,b=1)|\psi_3(t=0)\rangle$. The parameters are taken as $\sigma_{12}=\sigma_{23}=1.365$, $\sigma_{12r}=\sigma_{23r}=10^3$, $a=2$ and $b=1$ ($k_1=1$, $k_2=0$). The fidelity is $F(t=0)\approx0.5005$. The input state $|\psi_1\rangle$ is the two-mode state of Eq. (2.1). The parameters of $|\psi_1\rangle$ are the same as those of Fig. 1. The units are atomic units.
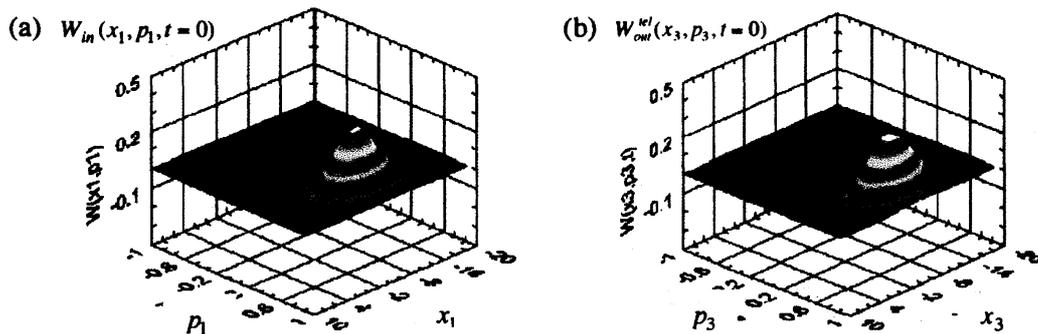
Fig. 8 (a) The Wigner distribution $W_{in}(x_1,p_1,t=0)$ of the one-mode input state $|\psi_1(t=0)\rangle=|\phi_1^+(t=0)\rangle$. The parameters of $|\phi_1^+(t=0)\rangle$ are the same as those of Fig. 1. (b) The Wigner distribution $W_{out}^{tel}(x_3,p_3,t=0)$ of the output state $|\psi_3^{tel}(t=0)\rangle=\hat{U}(a=2,b=1)|\psi_3(t=0)\rangle$ for the one-mode input state $|\psi_1(t=0)\rangle=|\phi_1^+(t=0)\rangle$. The parameters are taken as $\sigma_{12}=\sigma_{23}=1.365$, $\sigma_{12r}=\sigma_{23r}=10^3$, $a=2$, $b=1$ ($k_1=1,k_2=0$). The fidelity is $F(t=0)=0.964$. The units are atomic units.

4. Summary

We have presented a time-dependent model that explicitly describes teleportation of an unknown quantum state of the position and momentum of a particle with mass. The model is based on the Schrödinger equation and hence nonrelativistic. The model describes, in free space, the time-evolution of the post-measurement state generated at Bob's site. We illustrated how such time-evolution of the post-measurement state causes inefficiency of teleportation.

We also discussed how an optimal teleportation with a high degree of fidelity and a high probability is possible. As a special case, we illustrated a situation where one of the two modes of the input state is transferred to another mode by the teleportation. We discussed such a situation in connection with the classical limit of quantum teleportation.

Acknowledgments

References

[1] C. H. Bennett, Brassard, C. Crepeau, R. Jozsa, A. Peres, and W. K. Wootters, Phys. Rev. Lett. **70**, 1895 (1993).

[2] L. Vaidman, Phys. Rev. Lett. **49**, 1473 (1994).

[3] A. Einstein, B. Podolsky and N. Rosen, Phys.Rev. **47**, 777 (1935).

[4] S. L. Braunstein and H. J. Kimble, Phys. Rev. Lett. **80**, 869 (1998);
Edited by D. Bouwmeester, A. Ekert and A. Zeilinger, in *The Physics of Quantum Information* (Springer, 2000), pp.77-87.

[5] A. Furusawa, J. L. Sorensen, S. L. Braunstein, C. A. Fuchs, H. J. Kimble, E. J. Polzik, *Science* **282**, 706 (1998).

[6] E. Wigner, Phys. Rev. **40**, 749 (1932).